MODELLING OF PROGRESSIVE MATRIX CRACKING INDUCED DELAMINATIONS USING AN ENRICHED SHELL ELEMENT FORMULATION

Johannes Främby[1*], Martin Fagerström[1] and Jim Brouzoulis[2]

[1] Department of Industrial and Materials Science, Division of Material and Computational Mechanics, Chalmers University of Technology, Gothenburg, Sweden,
[2] Department of Mechanics and Maritime Sciences, Division of Dynamics, Chalmers University of Technology, Gothenburg, Sweden.
[*]Corresponding author: johannes.framby@chalmers.se

Keywords: Adaptive shell, XFEM, Delamination, MCID

ABSTRACT

In this contribution we present a computational model, implemented as an LS-DYNA user element, which can be adaptively refined through the thickness when and where delaminations need to be represented during a simulation. Using this we have investigated the models capability of simulating Matrix Crack Induced Delaminations (MCID), which it has been found to do well. Special emphasis has been put on the potential issue arising when combining smeared intralaminar cracks with explicitly modelled interlaminar cracks by cohesive interface elements, as is done in our model. We have found that this seems to be of small practical importance, especially when the element size is small, which normally is the case when modelling delaminations using cohesive interface elements.

1. INTRODUCTION

To meet the increasing demands from regulatory bodies on CO_2 emissions from automotive cars, the automotive industry is currently very active in reducing vehicle weight, where one significant step is to increase the amount of laminated composites made from Fibre Reinforced Polymers (FRPs) due to their superior specific properties (*e.g.* specific strength and specific energy absorption) compared to conventional metals. However, the development of numerical finite element (FE) tools for the accurate prediction of the crash response of vehicle structures in FRPs are crucial for structural composites to have a widespread use in future cars.

In order to achieve good deformation predictions of structural composite components in *e.g.* automotive crash and durability simulations, a proper modelling of the delamination process is crucial. Besides being a result of high interlaminar transverse (out-of-plane) stresses, delaminations are commonly initiated from stress concentrations at the tips of transverse matrix cracks, so-called matrix crack induced delaminations (MCID), illustrated in Figure 1.

In general, in order to capture delamination initiation and growth, detailed modelling of each ply by separate elements and interconnecting cohesive interface elements is required. However, due to restrictions on the simulation time, such high-fidelity models are not feasible to use in industrial applications such as full vehicle crash simulations. Therefore, in an attempt to achieve predictive and yet computationally efficient modelling of delamination initiation and growth, an adaptive enrichment methodology for the modelling of multiple and arbitrarily located delamination cracks using an equivalent single-layer (ESL) shell model has recently been presented [1]. The methodology has been shown to save substantial amounts of computational efforts, thus having the potential to enable industrial simulations of progressive delamination failure in composite structures. However, up until recently, the methodology has not been able to capture the crucial mechanism of MCID.

2. ADAPTIVE COMPUTATIONAL MODEL

The methodology presented in [1] is based on an enriched shell element formulation [2] where arbitrarily many delamination cracks can be modelled using only one element through the thickness. In summary the methodology consists of the following steps: *i*) The laminated structure is initially

represented by a single layer of shell elements through the thickness; *ii*) areas in which delaminations are expected to initiate are predicted and *iii*) the associated elements are locally refined through the thickness by introducing delamination enrichments and associated cohesive interfaces; *iv*) If the initiated delaminations propagate, the enrichment areas are expanded such that the fracture process can be accurately resolved. This enables to capture propagating delaminations in the structure, but only when and where it is needed.

In order for the model to behave correctly the areas where delaminations are critical must be predicted. In [1] these areas where predicted by high interlaminar transverse (out-of-plane) stresses, estimated using a stress recovery method. However, other initiators such as MCID was not considered.

2.1 Modelling Matrix Cracked Induced Delaminations

Ideally, the intralaminar matrix cracks should be explicitly modelled such that the cohesive interface representing the delamination crack is split at the intralaminar crack tip. This way the interface tractions can develop correctly if the delamination wants to propagate, Figure 2(a). This can be achieved by either designing the mesh to follow the fibre direction or by local enrichment of the element, as made by [3]–[5]. However, in our proposed model the intralaminar cracks are not explicitly modelled but instead represented by a material model which smears the crack within the ply element, similar to that in [6]. The reason do so is because the, often numerous, intralaminar cracks do not need to be represented by individual degrees of freedom (DOFs) and it allows for arbitrary mesh and fibre directions. A negative consequence is that the kinematics of the intersecting intralaminar crack and interlaminar interface is not represented correctly, Figure 2(b).

To remedy the potential issues of combining a smeared crack intralaminar model with an interlaminar cohesive interface there are several options to explore. As one option, one could make an internal split of the cohesive interface element, where it is assumed that the entire (smeared) crack jump is applied to the split of the interface, cf. Figure 2(c). This would neglect any elastic effect in the plies and require the additional storage of integration point data since two, instead of one, cohesive element are used in the interface.

However, in this work, we instead propose two simpler options to address the issue: *i*) in the case of an intralaminar crack, we do not use any interface element directly above the crack or *ii*) we do not address the problem at all. The former alternative would enable better representation of the delamination kinematics by the cohesive interface in vicinity of the crack but also neglect the energy dissipated by the removed interface element, especially if the in-plane size of the element is large. However, this contribution to the energy dissipation can be calculated a priori and can therefore be added to the intralaminar fracture energy if needed. The latter option would potentially underestimate the initial propagation of the delamination caused by delayed interface damage evolution due to that the shear sliding would be constrained from the bottom (in this case) by the lack of non-explicit kinematical representation of the matrix crack. However, in the context of large deformations this initial error is expected to be of small influence.

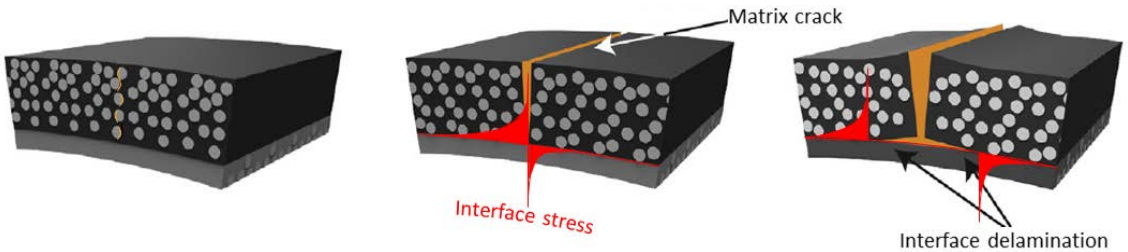

Figure 1: Matrix Crack Induced Delamination: (a) A transverse matric crack has initiated and can eventually grow into (b) a fully developed crack. If the crack meets an interface where delaminations can grow (e.g. a ply with considerably different fibre angle) high transverse stress concentrations will result in the intersection of the interface and the crack tip. (c) These stresses can then drive the formation of a delamination. Adapted from [7].

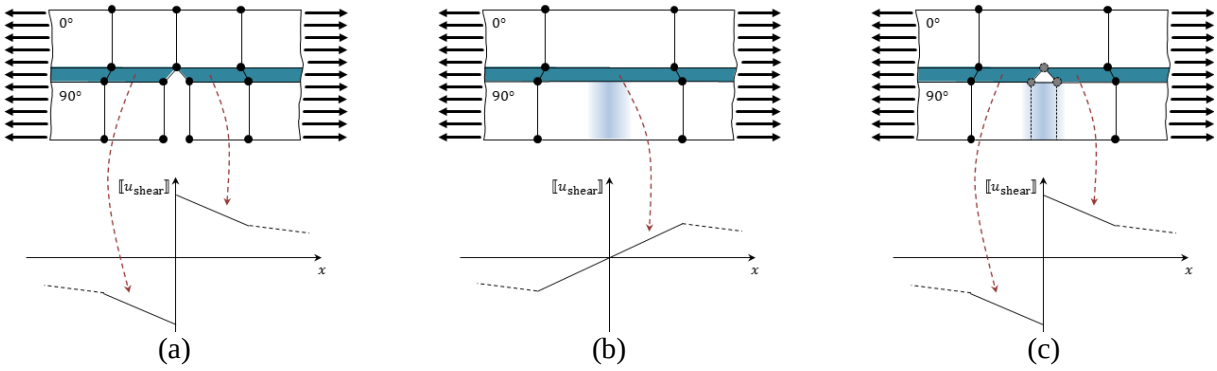

Figure 2: Strategies for modelling interaction between intra- and interlaminar cracks by: (a) explicitly modelling the intralaminar matrix crack and division of the cohesive element; (b) smeared intralaminar crack and no treatment of the cohesive element and (c) smeared intralaminar crack and internal division of the cohesive element by imposing the (intralaminar) crack jump on the element.

2.2 Implementation in LS-DYNA

Our adaptive methodology [1], previously implemented in the open source software OOFEM [8], is currently being implemented as a user element in the commercial FE solver LS-DYNA [9], a well-accepted industry tool for performing automotive crash simulations.

There are some differences between the LS-DYNA and the OOFEM implementations. For example, the OOFEM implementation was based on a thin 7-DOF mid-surface shell element where the delamination enrichments where introduced using the eXtended Finite Element Method (XFEM) [10], [11]. Instead the LS-DYNA implementation is based on a solid shell element (eight nodes with only translational DOFs) where the delaminations are represented using internal sub-elements, so called Augmented FEM (AFEM) [12]. These are subtle differences and we stated already in [1] that the adaptive methodology is not dependent on the choice of either element formulation or enrichment technique, but that the key idea is that the delamination DOFs are introduced during the simulation.

Besides these differences, development in OOFEM enabled full freedom to introduce any number of additional enrichment DOFs and the management of these could be handled by an overhead function. Unfortunately, this is not the case in LS-DYNA, where the management of enrichment DOFs must for a feasible computational effort be controlled by the element themselves and there is (at the moment) a hard-wired limit on the amount of extra DOFs, allowing only five internal delaminations per user element. However, the choice of using a solid shell element formulation as basis enables the possibility to stack several user elements on top of each other in order to represent more delaminations if necessary. Furthermore, the lack of a management function means that, at the moment, we cannot limit the enrichment patch in-plane, with the implication that when an element is refined this affects all the user elements sharing the same part.

In Figure 3 we try to illustrate the structure of the LS-DYNA user element. Externally, the element is an eight-node solid, with one integration point (IP) through the thickness for each laminate layer. By assigning global extra DOFs to represent the internal interface(s), the element can be sub-divided internally into sub-elements connected by cohesive interface elements. The layer IPs are then assigned to the appropriate sub-element. Both the undivided element and the sub-elements are modelled using LS-DYNA thick shells (element form 3) and the cohesive interfaces using LS-DYNA eight-node cohesive element (element form 19).

A more profound difference between the OOFEM and the LS-DYNA implementations is that in OOFEM we considered quasi-static problems, which were solved using an iterative (implicit) solver. However, in LS-DYNA we are solving a dynamic problem using a central difference (explicit) time stepping solution scheme. This has the effect that there is no guaranteed balance of momentum and one has to make sure that the incremental steps are smaller than the critical time step.

While this a known drawback with explicit solvers this further complicates the adaptive introduction of delaminations enrichments. With the implicit, solver the solution could be found even

if the element refinement disturbed the problem. However, in a dynamic problem solved with an explicit solver there is a large risk of introducing unphysical oscillations when refining the element, as concluded in [13]. This issue will be further addressed below.

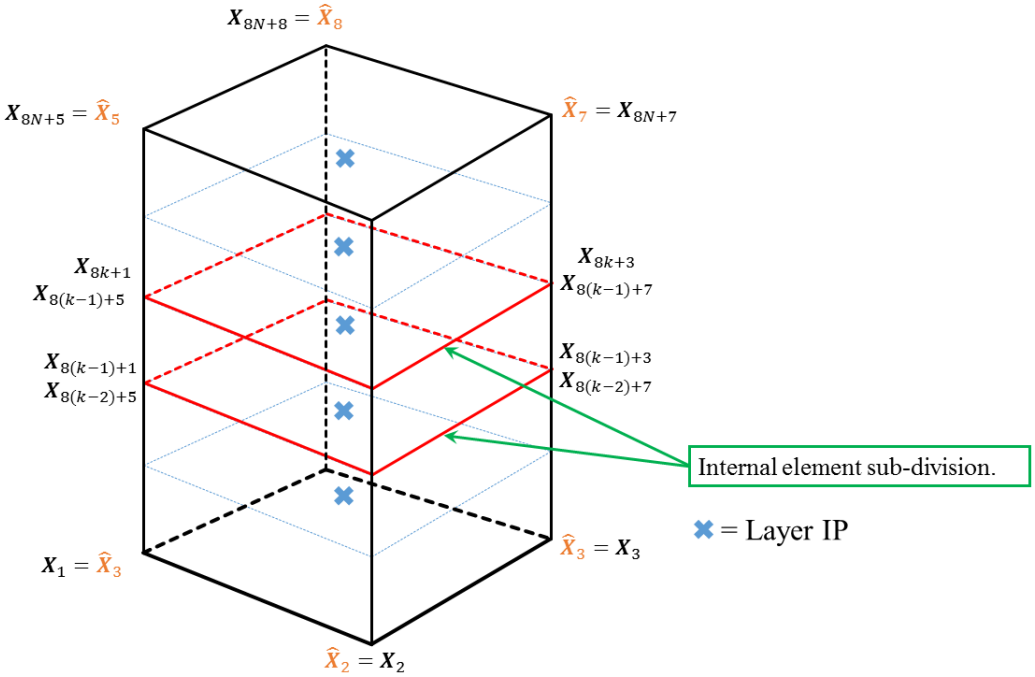

Figure 3: Illustration of structure of the LS-DYNA user element. $\hat{\boldsymbol{X}}_i$ represent the coordinates of the eight standard nodes, while $\boldsymbol{X}_i$ represent all nodes used in the element and their global numbering (exemplified for an arbitrary layer k). N is the total number of interface sub-divisions in the element.

3 NUMERICAL EXAMPLES

To illustrate our proposed model's ability to simulate MCID we will reproduce one of the numerical examples in [5] where they simulated the four point bending experiment performed by Mortell *et al.* [7]. The beam considered is illustrated in Figure 3, where we indicate that the bottom eight layers are modelled using our user element while the remaining seven layers are modelled using LS-DYNA thick shell (element form 3). Following the findings in [7], five positions of the bottom 90°-layers of the beam, evenly distributed in the load span, are modelled with a smeared crack material model representing the matrix cracks (cf. Figure 4). Upon damage evolution all stress components (including the fibre direction) are degraded. The rest of the beam is modelled as an orthotropic linear elastic material, thus final failure of the beam when the 0°-layers should fail is not included. Only delamination of the bottom 90°/0°-interface is considered.

The ply material is HTA/6376, whose material properties are summarised in Table 1, where it should be noted that the interface strengths have been reduced by 80% in order to allow an element in-plane length of 0.25 mm (found through simulations and strategies from [14]).

To compare the results from the user element we will compare the force vs. displacement curves from the experiment as well as the Local Delamination Ratio (LDR) in [7]. LDR compares the length of an individual delamination e to the through-thickness height h of the transverse intralaminar crack which initiated the delamination (cf. Figure 6):

$$\text{LDR} = \frac{e}{h}. \tag{1}$$

Finally we also make a comparison to two simulation models in which also the bottom layers are modelled using LS-DYNA thick shells (four layers in each element). The difference between these two models is that the cohesive interface has been removed at the crack positions (as indicated in Figure 3) in one of them.

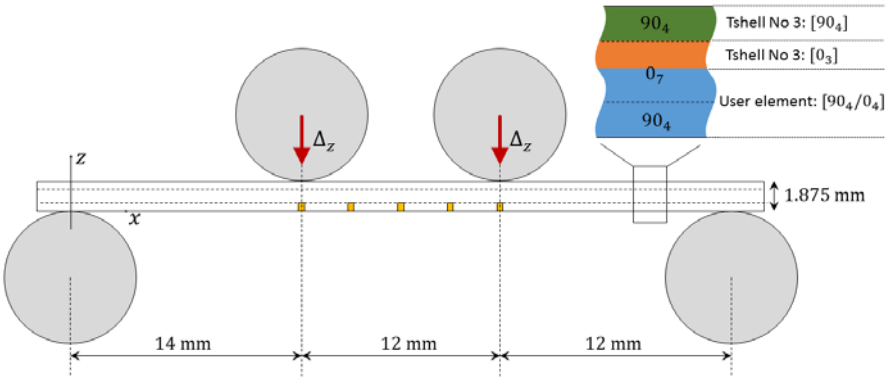

Figure 4: Four point bending example from [7]. The orange squares in the bottom 90-layers indicate the positions of the intralaminar cracks. The load pins have a radius of 4 mm.

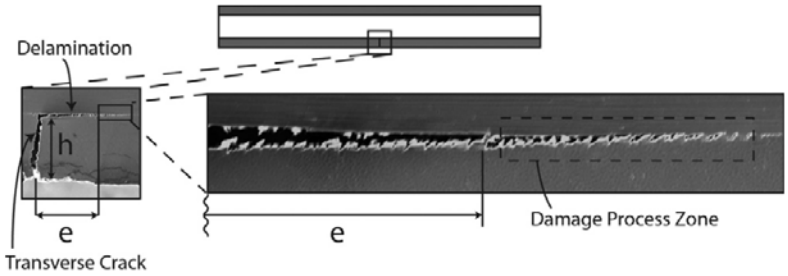

Figure 5: Illustration of through-thickness height h of the intralaminar crack and the delamination length e used to calculate Local Delamination Ratio in (1) as defined in [7]. © 2014 Elsevier Ltd.

Engineering constant	Unit	Value
E_1	[GPa]	140
E_2, E_3	[GPa]	10
G_{12}, G_{13}	[GPa]	5.2
G_{23}	[GPa]	3.9
ν_{21}, ν_{31}	–	0.0214
ν_{32}	–	0.5
K^*	[N/mm^2]	10^6
$N^\dagger$	[MPa]	21
$S^\dagger$	[MPa]	28
G_{Ic}	[J/m^2]	432
G_{IIc}*	[J/m^2]	1002

Table 1: Material data for HTA/6376 from [5].

3.1 Load-displacement response

In Figure 6, the force response is plotted versus displacement of the load pins for the four different simulation models of the four point beam example. All models show a response in between the two experimental results from [7], however with some variation in degree of oscillations. In all cases the intralaminar cracks are fully developed at approximately 100 N and the curves for the two reference models and the user element with initial refinement split are very similar. The effect of having a cohesive interface above the intralaminar matrix crack or not seems almost negligible.

* Assumed values.
† Strength values scaled by 80%.

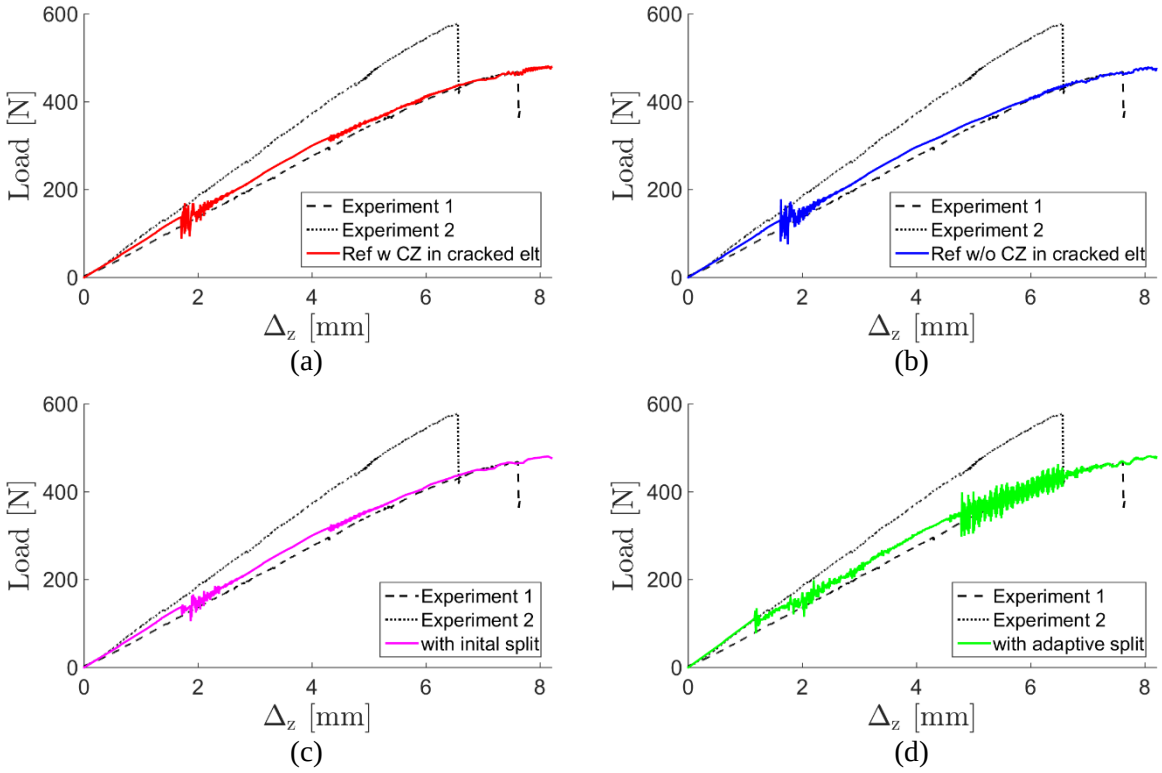

Figure 6: Load-displacement response of the four models; (a) the reference model with a cohesive interface above the intralaminar crack, (b) the same reference model but without a cohesive interface above the intralaminar crack, (c) the user element model with refinement split present from the start of the simulation and (d) the user element model with the refinement inserted when the intralaminar damage onset criterion reaches 70 %. Experimental curves from [7].

3.2 Damage evolution in the cohesive interface

In order to compare the evolution of the delamination cracks the damage of the lower 90°/0°-interface in the beam is plotted in Figure 7 for the different simulation models. The three first plots show delaminations being initiated from the intralaminar cracks. However, in the case of adaptive refinement the interface shows an unphysical damage pattern.

In Figure 8 the LDR is plotted against load pin displacements for the delaminations within the load span (*i.e.* the two outward delaminations have been excluded), where we can see that the first reference model and the user-element with initial refinement split show the same delamination evolution. For the simulation models the delamination length e is calculated as the integral of the damage in a delamination times the element in-plane length. This means that a half damaged interface element would result in a contribution of 0.5 × 0.25 mm to the e-value in (1) even though it is not fully damaged. This could explain why the LDR in the simulations start earlier compared to that of the experiment. In addition, it should also be noted that the experimental LDR-curves are taken from only one of the experiments (No. 1 in Figure 6).

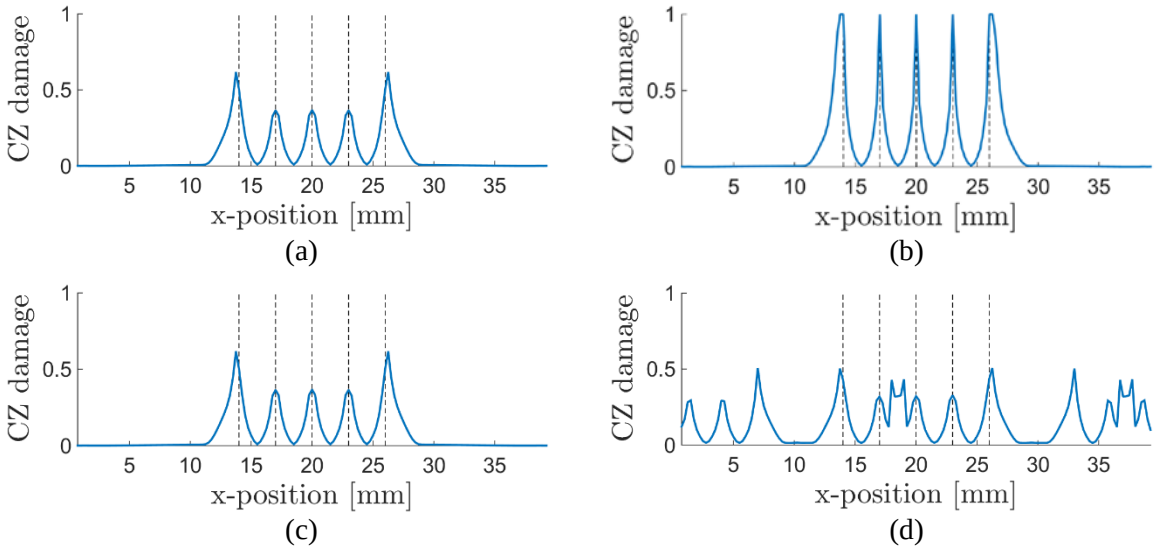

Figure 7: Damage in the cohesive interface at a load pin displacement of 4 mm in the two reference models (a-b) and the two user element models (c-d). NB: the non-present cohesive interfaces in the second reference models are indicated as fully damaged. The dashed lines indicate the matrix cracks.

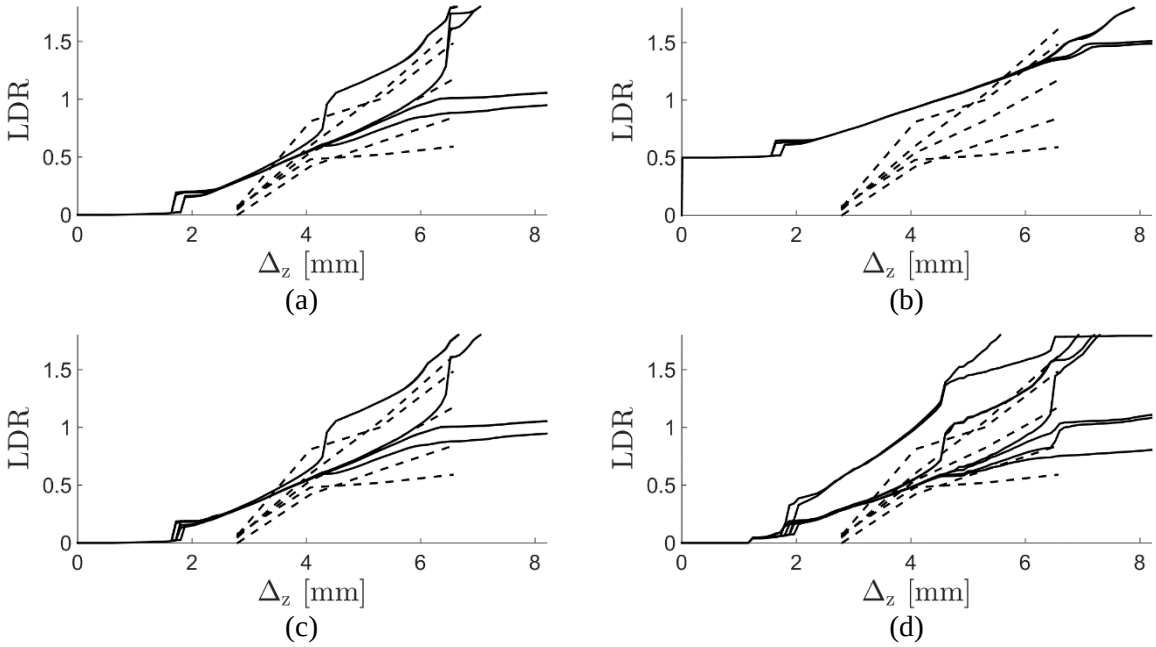

Figure 8: Local delamination ratio (LDR) for the delaminations in the load span plotted against load pin displacements for the two reference models (a-b) and the two user element models (c-d).

4 CONCLUSIONS

In this contribution we have presented a computational model which can be adaptively refined through the thickness when and where delaminations need to be represented during a simulation. The model combines a smeared intralaminar crack material model with interlaminar cohesive interface elements and is currently being implemented as an LS-DYNA user element.

We have investigated the models ability to simulate MCID, by comparing its response to both a reference model and to experimental results and found this to be successful. Especially, we have addressed the potential issue of combining smeared intralaminar cracks with explicitly modelled interlaminar cracks by cohesive interface elements and found that this seems to be of small practical importance. However, it should be emphasised that the in-plane element size is approximately a tenth

to those usually used in industrial crash simulations, which is the intended application of the presented model. Hence, the effect of one cohesive element behaving incorrectly is small. From computational cost point of view it would be beneficial to use larger elements, however, the size is severely limited if the cohesive fracture process is to be modelled correctly [14]. If larger element sizes can be achieved, the issue of smeared crack with intralaminar cohesive interfaces should thus be re-addressed.

At the moment the model is rather unstable when it is adaptively refined during simulation, resulting in unphysical damage evolution. A possible remedy for this is to extend the refinement process over longer time as suggested by [13], which will be addressed in the near future.

ACKNOWLEDGEMENTS

The current work has been funded by the Swedish Strategic Vehicle Research and Innovation Programme on Vehicle and Traffic Safety via the project *Modelling crash behaviour in future lightweight composite vehicles – Step 2*, which is gratefully acknowledged. The simulations were performed on resources provided by the Swedish National Infrastructure for Computing (SNIC) at Chalmers Centre for Computational Science and Engineering (C3SE)

REFERENCES

[1] J. Främby, M. Fagerström, and J. Brouzoulis, “Adaptive modelling of delamination initiation and propagation using an equivalent single-layer shell approach,” *Int. J. Numer. Methods Eng.*, vol. 0, pp. 1–30, 2017.

[2] J. Brouzoulis and M. Fagerström, “An enriched shell element formulation for efficient modeling of multiple delamination propagation in laminates,” *Compos. Struct.*, vol. 126, pp. 196–206, 2015.

[3] X. J. Fang, Q. D. Yang, B. N. Cox, and Z. Q. Zhou, “An augmented cohesive zone element for arbitrary crack coalescence and bifurcation in heterogeneous materials,” *Int. J. Numer. Methods Eng.*, vol. 88, no. 9, pp. 841–861, 2011.

[4] B. Y. Chen, S. T. Pinho, N. V. De Carvalho, P. M. Baiz, and T. E. Tay, “A floating node method for the modelling of discontinuities in composites,” *Eng. Fract. Mech.*, vol. 127, pp. 104–134, 2014.

[5] J. Reiner, M. Veidt, M. Dargusch, and L. Gross, “A progressive analysis of matrix cracking-induced delamination in composite laminates using an advanced phantom node method,” *J. Compos. Mater.*, p. 21998316684203, 2016.

[6] S. T. Pinho, L. Iannucci, and P. Robinson, “Physically based failure models and criteria for laminated fibre-reinforced composites with emphasis on fibre kinking. Part II: FE implementation,” *Compos. Part A Appl. Sci. Manuf.*, vol. 37, no. 5, pp. 766–777, 2006.

[7] D. J. Mortell, D. A. Tanner, and C. T. McCarthy, “In-situ SEM study of transverse cracking and delamination in laminated composite materials,” *Compos. Sci. Technol.*, vol. 105, pp. 118–126, 2014.

[8] B. Patzák, “OOFEM,” 2000. [Online]. Available: www.oofem.org. [Accessed: 25-Apr-2017].

[9] LSTC, “LS-DYNA,” 2011. [Online]. Available: lstc.com. [Accessed: 10-Jun-2017].

[10] T. Belytschko and T. Black, “Elastic crack growth in finite elements with minimal remeshing,” *Int. J. Numer. Methods Eng.*, vol. 45, no. 5, pp. 601–620, 1999.

[11] N. Moës, J. Dolbow, and T. Belytschko, “A finite element method for crack growth without remeshing,” *Int. J. Numer. Methods Eng.*, vol. 46, no. 1, pp. 131–150, 1999.

[12] W. Liu, Q. D. Yang, S. Mohammadizadeh, and X. Y. Su, “An efficient augmented finite element method for arbitrary cracking and crack interaction in solids,” *Int. J. Numer. Methods Eng.*, vol. 99, no. 6, pp. 438–468, 2014.

[13] S. Mostofizadeh, M. Fagerström, and R. Larsson, “Dynamic crack propagation in elastoplastic thin-walled structures: Modelling and validation,” *Int. J. Numer. Methods Eng.*, vol. 96, no. 2, pp. 63–86, 2013.

[14] A. Soto, E. V. González, P. Maimí, A. Turon, J. R. Sainz de Aja, and F. M. de la Escalera, “Cohesive zone length of orthotropic materials undergoing delamination,” *Eng. Fract. Mech.*, vol. 159, pp. 174–188, 2016.